

J E P T

Edited by: DGO-Fachausschuss Forschung – Hilden / Germany

Allium sativum (Garlic) as green corrosion inhibitor for low carbon steel in HCl solutions

The use of allium sativum (garlic) as a green inhibitor for the corrosion of low carbon steel in 1M HCl has been studied using potentiodynamic polarization, electrochemical impedance spectroscopy (EIS), electrochemical frequency modulation (EFM) techniques and weight loss measurements. Allium sativum has been proved to be good inhibitor. This reduction in the corrosion rate was due to the formation of an external layer formed by S-containing film present in the extract which was adsorbed physically on the metal surface. Allium sativum acted as a mixed type of inhibitor. The inhibition efficiency increases with increasing the inhibitor concentration, but decreases with raising the temperature. The adsorption of allium sativum on the metal surface follows Temkin's adsorption isotherm. From EFM the causality factors are very close to theoretical values which...

Received: 2015-01-25

Received in revised form: 2015-03-26

Accepted: 2015-03-30

Keywords:

low Carbon steel, green inhibitor, acidic corrosion

Authors:

A. S Fouda, A. A. Attia
and S. M. Ghoneim

DOI:

10.12850/ISSN2196-0267.JEPT4166

Table of contents

1. Introduction	4
2. Experimental	5
2.1. Composition of material samples	5
2.2. Solutions	5
2.3. Weight loss measurements	5
2.4. Electrochemical measurements	5
2.5. Surface examinations	6
3. Results and Discussion	7
3.1. Chemical Method (Weight-loss measurements)	7
3.2. Effect of Temperature	7
3.3. Adsorption Isotherm	7
3.4. Kinetic –thermodynamic corrosion parameters	9
3.5. Potentiodynamic polarization measurements	10
3.6. Electrochemical impedance spectroscopy (EIS) measurements	11
3.7. Electrochemical frequency modulation (EFM) measurements	11
3.8. Surface morphology	12
4. Mechanism of Corrosion Inhibition	14
5. Conclusion	15
References	16
Authors	18

Allium sativum (Garlic) as green corrosion inhibitor for low carbon steel in HCl solutions

A. S. Fouda^{1*}, A. A. Attia², and S. M. Ghoneim¹

¹Department of Chemistry, Faculty of Science, El-Mansoura University, El-Mansoura-35516, Egypt Email: asfouda@hotmail.com

²Department of Chemistry, Faculty of Science, Zagazig University, Zagazig, Egypt Email: azzattia91@yahoo.com; drarara97@yahoo.com

*Corresponding author

The use of allium sativum (garlic) as a green inhibitor for the corrosion of low carbon steel in 1M HCl has been studied using potentiodynamic polarization, electrochemical impedance spectroscopy (EIS), electrochemical frequency modulation (EFM) techniques and weight loss measurements. Allium sativum has been proved to be good

inhibitor. This reduction in the corrosion rate was due to the formation of an external layer formed by S-containing film present in the extract which was adsorbed physically on the metal surface. Allium sativum acted as a mixed type of inhibitor. The inhibition efficiency increases with increasing the inhibitor concentration, but decreases with raising the temperature. The adsorption of allium sativum on the metal surface follows Temkin's adsorption isotherm. From EFM the causality factors are very close to theoretical values which indicate that the measured data are of good quality. Nyquist plots show a single capacitive loop in uninhibited and inhibited solutions.

Keywords: low Carbon steel, green inhibitor, acidic corrosion

Paper: Received: 2015-01-25 / Received in revised form: 2015-03-26 / Accepted: 2015-03-30

DOI: 10.12850/ISSN2196-0267.JEPT4166

1. Introduction

Corrosion control of metal is of technical, economical, environmental and aesthetical importance. The use of inhibitor is the best way to prevent metal and alloys from corrosion. There is an intensive effort underway to develop new plant origin corrosion inhibitors for metal subjected to various environmental conditions. Green corrosion inhibitors are biodegradable and don't contain heavy metals or other toxic compounds. Some research groups have reported the successful use of naturally occurring substances to inhibit the corrosion of metals in acidic and alkaline environ-

ment. Several reports are available on the various natural products used as green inhibitors. The use of plant extracts like the aqueous extract of Fenugreek leaves [1]; *Calendula Officinalis* flower [2]; aqueous extract of Olive leaves [3]; *Sansevieria Trifasciata* extract [4]; Mangrove tannins and their flavanoid monomers [5]; *Ocimum Basilicum* extract [6]; and ficus extract [7] have been studied. Also, Obot et al. [8] and Umoren et al. [9] have studied ginseng root and *Raphia hookeri*, *Vigna Unguiculata* [10] and exudate gum from *Dacryodes Edulis* [11], and established their corrosion inhibition effects. They were all found to be good corrosion inhibitors with no effect on the environ-

ment. In spite of the broad spectrum of inhibitors chosen from organic compounds, it is significant to note that the search for corrosion inhibitors that have optimum efficiency is still going on [12]. The aim of the present work therefore is to assay the phytochemicals present in *Allium sativum* and investigate its inhibitive properties on low carbon steel by chemical and electrochemical techniques at different temperatures.

Preparation of plant Extract

Plant materials were dried in the shade at room temperature, ground using electrical mill into fine powder then mix 20 grams of *allium sativum powder* with 200 ml of ethanol 70% and leave the solution with constant stirring using shaker for 24 hours in a room temperature, after that the solution was left open to air at room temperature to dry and all ethanol was evaporated. After that, one gram of the solid was weighted and dissolved in 1000 ml of bidistilled water. The stock solution was used to prepare the desired concentrations by dilution.

2. Experimental

2.1. Composition of material samples

See table 1.

2.2. Solutions

The aggressive solutions, 1 M HCl solutions were prepared by dilution of analytical grade (37 %) HCl with bi-distilled water.

2.3. Weight loss measurements

Seven parallel low carbon steel sheets of $2 \times 2 \times 0.2$ cm were abraded with different grades of emery paper up to 1200 and then washed with bi-distilled water and acetone. After accurate weighing, the specimens were immersed in a 100 ml HCl with and without addition of different concentrations of *allium sativum*. All the aggressive acid solutions were open to air. After 3 h, the specimens were taken out, washed, dried, and weighed accurately. The average weight loss of the seven parallel α -brass sheets could be obtained. The inhibition efficiency (%IE) and the degree of surface coverage (Θ) of investigated extract for the corrosion of low carbon steel in HCl were calculated from equation (1) [13]:

Equation 1:

$$\% \text{IE} = \Theta \times 100 = [1 - (W / W^{\circ})] \times 100$$

where W° and W are the values of the average weight losses without and with addition of the inhibitor, respectively.

2.4. Electrochemical measurements

Electrochemical experiments were performed using a typical three-compartment glass cell consisted of the low carbon steel specimen as working electrode (1 cm^2), saturated calomel electrode (SCE) as a reference electrode and a platinum foil (1 cm^2) as a counter electrode. The reference electrode was connected to a Luggin capillary and the tip of the Luggin capillary is made very close to the surface of the working electrode to mini-

Tab. 1: Chemical composition (weight %) of the low carbon steel

Elements	C	Cr	Ni	Si	Mn	P	S	Fe
Composition (weight %)	0.14 – 0.20	0.1	0.01	0.24	0.5	0.05	0.05	rest

mize IR drop. All the measurements were done in solutions open to atmosphere under unstirred conditions. All potential values were reported versus SCE. Prior to every experiment, the electrode was abraded with successive different grades of emery paper, degreased with acetone and washed with bi-distilled water and finally dried. Tafel polarization curves were obtained by changing the electrode potential automatically from (- 0.5 to 0.5 V vs. SCE) at open circuit potential with a scan rate of 1 mVs⁻¹. Stern-Geary method [14] used for the determination of corrosion current is performed by extrapolation of anodic and cathodic Tafel lines to a point which gives log i_{corr} and the corresponding corrosion potential (E_{corr}) for extract free acid and for each concentration of extract. Then i_{corr} was used for calculation of inhibition efficiency (%IE) and surface coverage (θ) from equation (2):

Equation 2:

$$\%IE = \theta \times 100 = [1 - (i_{corr(inh)} / i_{corr(free)})] \times 100$$

Where $i_{corr(free)}$ and $i_{corr(inh)}$ are the corrosion current densities in the absence and presence of extract, respectively.

Impedance measurements were carried out in frequency range from 100 kHz to 0.1Hz with amplitude of 5 mV peak-to-peak using ac signals at open circuit potential. The experimental impedance was analyzed and interpreted based on the equivalent circuit. The main parameters deduced from the analysis of Nyquist diagram are the resistance of charge transfer R_{ct} and the capacitance of double layer C_{dl} . The inhibition efficiencies (%IE) and the surface coverage (θ) obtained from the impedance measurements are defined by equation (3):

Equation 3:

$$\%IE = \theta \times 100 = [1 - (R_{ct}^{\circ} / R_{ct})] \times 100$$

where R_{ct}° and R_{ct} are the charge transfer resistance in the absence and presence of inhibitor, respectively.

Electrochemical frequency modulation, EFM, was carried out using two frequencies 2 and 5 Hz. The base frequency was 0.1 Hz, so the wave form repeats after 1 s. The higher frequency must be at least two times the lower one. The higher frequency must also be sufficiently slow that the charging of the double layer does not contribute to the current response. Often, 10 Hz is a reasonable limit. The Intermodulation spectra contain current responses assigned for harmonical and intermodulation current peaks. The larger peaks were used to calculate the corrosion current density (i_{corr}), the Tafel slopes (β_a and β_c) and the causality factors CF-2& CF-3 [15, 16].

The electrode potential was allowed to stabilize for 30 min before starting the measurements. All the experiments were conducted at 25°C. The results were always repeated at least three times to check the reproducibility.

Measurements were performed using Gamry Instrument Potentiostat/ Galvanostat/ ZRA (PCI4-G750). This includes a Gamry framework system v 6.03 Gamry applications include DC105 software for DC corrosion measurements, EIS300 software for electrochemical impedance spectroscopy measurements and EFM140 for electrochemical frequency modulation measurements along with a computer for collecting data. Echem analyst v 6.03 software was used for plotting, graphing, and fitting data.

2.5. Surface examinations

The low carbon steel surface was prepared by keeping the specimens for 24hrs in 1M HCl in the presence and absence of extract, after abraded

using different emery papers up to 1200 grade size. Then, the specimens were washed gently with bi-distilled water, carefully dried and mounted into the spectrometer without any further treatment. The corroded low carbon steel surfaces were examined using an X-ray diffractometer Philips (pw-1390) with Cu-tube (Cu Ka1, $\lambda = 1.54051 \text{ \AA}$), a scanning electron microscope (SEM, JOEL, JSM-T20, Japan).

3. Results and Discussion

3.1. Chemical Method (Weight-loss measurements)

Figure 1 shows the weight loss-time curves for low carbon steel in 1M HCl in the presence and absence of different concentrations of *allium sativum* at 25°C. These curves are characterized by a sharp rise in weight loss from the beginning. Curves for additives containing system fall below that of the free acid. These curves indicated that, the weight loss of low carbon steel depends on the concentration of the extract. Increase in bulk concentration and consequently increase of surface coverage by the extract increases its inhibition efficiency towards low carbon steel dissolution. The results of Table 2 show that the

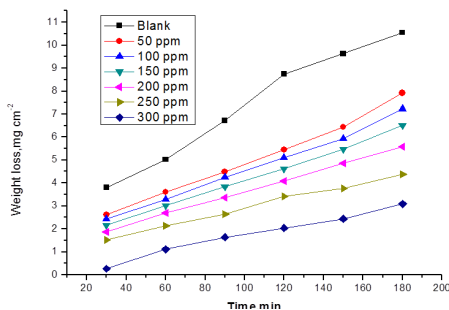


Fig.1: Weight loss-time curves for the corrosion of low carbon steel in 1 M HCl in the absence and presence of different concentrations of *allium sativum* at 25°C

Tab. 2: Values of inhibition efficiency (%IE) and surface coverage (θ) of *allium sativum* for the corrosion of low carbon steel in 1 M HCl at different concentrations and at 25°C

[Inh.] ppm	Allium sativum	
	θ	% IE
50	0.376	37.6
100	0.416	41.6
150	0.472	47.2
200	0.531	53.1
250	0.609	60.9
300	0.766	76.6

inhibition efficiency of the extract increases with the increase of its concentration in the corrosive medium. It is thus obvious that increase of bulk concentration and consequently, increase of surface area coverage by the extract retards the dissolution of low carbon steel.

3.2. Effect of Temperature

The effect of temperature on the corrosion rate of low carbon steel in 1M HCl and in presence of different extract concentrations was studied in the temperature range of 298–318K using weight loss measurements. As the temperature increases, the rate of corrosion increases and the inhibition efficiency of the extract decrease as shown in Table 3 for *allium sativum*. The adsorption behavior of extract on low carbon steel surface occurs through physical adsorption.

3.3. Adsorption Isotherm

One of the most convenient ways of expressing adsorption quantitatively is by deriving the adsorption isotherm that characterizes the metal/inhibitor/ environment system [17].

Tab. 3: Values of inhibition efficiency and corrosion rate (C.R) of allium *sativum* for low carbon steel in 1 M HCl at different concentrations and at different temperatures

[inh] ppm	298K		303K		308K		313K		318K	
	C.R	% IE	C.R	%IE	C.R	%IE	C.R	%IE	C.R	%IE
50	0.045	37.6	0.139	19.2	0.177	11.8	0.273	7.9	0.358	3.8
100	0.043	41.6	0.113	34.2	0.159	20.9	0.255	13.8	0.341	8.4
150	0.038	47.2	0.096	44.1	0.138	31.6	0.234	20.9	0.314	15.7
200	0.034	53.1	0.086	49.7	0.118	41.2	0.201	32.1	0.289	22.3
250	0.029	60.9	0.072	57.9	0.096	52.4	0.170	42.7	0.248	33.4
300	0.017	76.6	0.067	61.2	0.089	55.8	0.134	54.6	0.208	44.1

The surface coverage (θ) values were tested graphically to allow fitting of a suitable adsorption isotherm. Figure 2 shows the plot of $\log C$ vs θ which is typical of Temkin adsorption isotherm. Perfectly linear plot was obtained with higher regression constant. The Temkin isotherm is given as [18]:

Equation 4:

$$a\theta = \ln KC$$

where C is the inhibitor concentration and K_{ads} is the equilibrium constant of adsorption process and is related to the standard free energy of adsorption ($\Delta G^{\circ}_{\text{ads}}$) by equation (5):

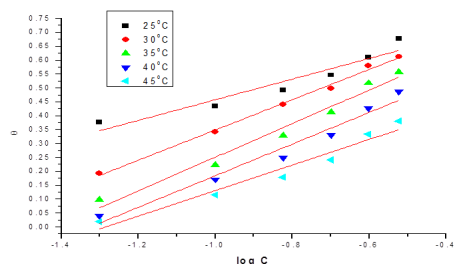


Fig.2: Temkin adsorption isotherm of *allium sativum* on low carbon steel surface in 1M HCl at different temperatures

Equation 5:

$$K_{\text{ads}} = 1/55.5 \exp(-\Delta G^{\circ}_{\text{ads}}/RT)$$

The value of 55.5 is the concentration of water in solution expressed in mole per liter, R is the universal gas constant and T is the absolute temperature. The calculated $\Delta G^{\circ}_{\text{ads}}$ values were also given in Table 4. The negative values of $\Delta G^{\circ}_{\text{ads}}$ ensure the spontaneity of the adsorption process and the stability of the adsorbed layer on the low carbon steel surface. It is well known that values of $\Delta G^{\circ}_{\text{ads}}$ of the order of -40 kJ mol^{-1} or higher involve charge sharing or transfer from the inhibi-

Tab. 4: Thermodynamic parameters for the adsorption of *allium sativum* on low carbon steel surface in 1 M HCl at different temperatures

$\Delta S^{\circ}_{\text{ads}}$ $\text{J mol}^{-1}\text{K}^{-1}$	$-\Delta H^{\circ}_{\text{ads}}$ kJ mol^{-1}	$-\Delta G^{\circ}_{\text{ads}}$ kJ mol^{-1}	K_{ads} M^{-1}	Temperature $^{\circ}\text{C}$
42.8	6.13	12.8	3.1	25
45.0		13.7	4.1	30
46.8		14.4	5	35
47.9		14.9	5.7	40
48.6		15.5	6.2	45

tor molecules to metal surface to form coordinate type of bond (chemisorption); those of order of -20 kJ mol^{-1} or lower indicate a physical adsorption [19, 20]. The calculated $\Delta G^{\circ}_{\text{ads}}$ values in Table 4 indicate that the adsorption mechanism of the investigated extract on low carbon steel in 1 M HCl solution is typical physical adsorption.

3.4. Kinetic–thermodynamic corrosion parameters

The effect of temperature (25 – 45°C) on the performance of the inhibitors at different concentrations of (50–300 ppm) for low carbon steel in 1M HCl was studied using weight-loss measurements. Plot of $\log k$ (corrosion rate) against $1/T$ (absolute temperature) Figure 3 for low carbon steel in 1M HCl, gave straight lines. The values of the slopes obtained at different temperatures permit the calculation of Arrhenius activation energy (E_a^*). Kinetic parameters for corrosion of low carbon steel were calculated from Arrhenius-type plot.

Equation 6:

$$k_{\text{corr}} = A \exp(-E_a^*/RT)$$

and transition state- type equation :

Equation 7:

$$k_{\text{corr}} = (RT/Nh) \exp(\Delta S^*/R) \exp(-\Delta H^*/RT)$$

where k is the rate of metal dissolution, h is Planck's constant, N is Avogadro's number, ΔS^* is the entropy of activation and ΔH^* is the enthalpy of activation. The relation between $\log k_{\text{corr}}$ vs. $1/T$ gives straight line, from its slope, ΔE^* can be computed. The relation between $\log k_{\text{corr}}/T$ vs. $1/T$ gives straight lines with slopes equal to $(\Delta H^*/2.303R)$ and intercepts equal to $[\log(R/Nh + \Delta S^*/2.303R)]$. Values of apparent activation parameters for corrosion of low carbon steel in 1 M HCl were shown in Table 5, without and with various concentrations

of *allium sativum*. The increase in E_a^* with increase inhibitor concentration Table 5 is typical of physical adsorption. The positive sign of the enthalpy (ΔH^*) reflects the endothermic nature of the low carbon steel dissolution process. Value of entropies (ΔS^*) imply that the activated complex at the rate determining step represents an association rather than a dissociation step, meaning that a decrease in disordering takes place on going from reactants to the activated complex. However, the value of (ΔS^*) decreases gradually with increasing inhibitor concentration in all the acid media.

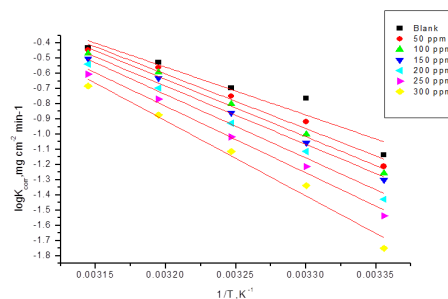


Fig.3: Plots of ($\log k_{\text{corr}}$) against ($1/T$) for low carbon steel in the presence and absence of *allium sativum* in 1 M HCl

Tab.5: Activation parameters for low carbon steel corrosion in the absence and presence of various concentrations of *allium sativum* in 1M HCl.

[inh] ppm	E_a^* kJ mol^{-1}	ΔH^* kJ mol^{-1}	$-\Delta S^*$ $\text{J mol}^{-1}\text{k}^{-1}$
blank	60.2	25.0	71.5
50	68.7	27.7	52.7
100	72.1	30.1	35.4
150	73.2	32.3	26.4
200	79.9	33.4	23.6
250	83.9	34.7	22.8
300	94.5	40.5	20.6

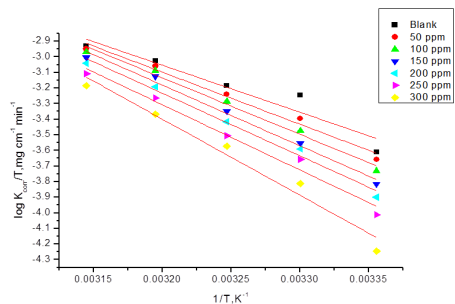


Fig.4: Plots of $\log k_{\text{corr}}/T$ against $1/T$ for low carbon steel in the presence and absence of *allium sativum* in 1 M HCl

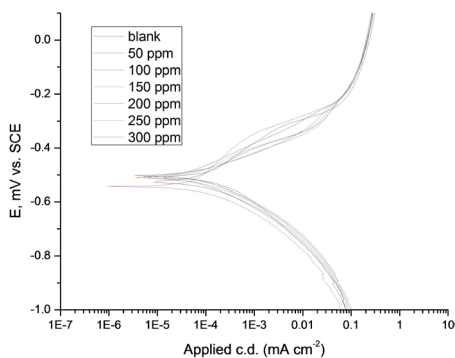


Fig.5: Potentiodynamic polarization curves for corrosion of low carbon steel in 1 M HCl in the absence and presence of different concentrations of *allium sativum* at 25°C

Tab.6: Corrosion potential (E_{corr}), corrosion current density (i_{corr}), Tafel slopes (β_c , β_a), degree of surface coverage (θ), and inhibition efficiency (% IE) of low carbon steel in 1 M HCl at 25°C for *allium sativum*

% IE	θ	C.R mpy	β_c mV dec ⁻¹	β_a mV dec ⁻¹	i_{corr} $\mu\text{A cm}^{-2}$	$-E_{\text{corr}}$ mV vs SCE	[inh.] ppm
----	----	142.4	147	152	312.0	508	Blank
34.9	0.349	92.9	186	123	203.0	502	50
67.3	0.673	46.7	189	122	102.0	508	100
68.1	0.681	45.4	119	82	99.4	502	150
71.0	0.710	41.3	118	107	90.4	542	200
77.1	0.771	32.7	98	99	71.6	510	250
78.4	0.784	30.7	75	115	67.3	526	300

3.5. Potentiodynamic polarization measurements

The potentiodynamic curves for low carbon steel in 1 M HCl in the absence and presence of *allium sativum* are shown in Figure 5. It is clear that; the investigated inhibitor affects the promoting retardation of anodic dissolution of low carbon steel and cathodic hydrogen discharge reactions. Electrochemical parameters such as corrosion current density (i_{corr}), corrosion potential (E_{corr}), Tafel constants (β_a and β_c), degree of surface coverage (θ) and inhibition efficiency (% η_p) were calculated from Tafel plots and are given in Table 6. It is observed that the presence of inhibitor lowers i_{corr} . It is also observed from Table 6 that E_{corr} values and Tafel slopes do not change significantly in inhibited solution as compared to uninhibited solution. The investigated extract does not shift the E_{corr} values significantly, suggesting that they behave as mixed type inhibitor [21]. Both cathodic (β_c) and anodic (β_a) Tafel lines are parallel and are shifted to more negative and positive direction, respectively by adding extract. This is indicating that the mechanism of the corrosion reaction does not change and the corrosion reaction is inhibited by simple adsorption mode [22].

The irregular trends of β_a and β_c values indicate the involvement of more than one type of species adsorbed on the metal surface.

3.6. Electrochemical impedance spectroscopy (EIS) measurements

EIS is well-established and it is powerful technique for studying the corrosion. Surface properties, electrode kinetics and mechanistic information can be obtained from impedance diagrams [23-26]. The effect of extract concentration on the impedance behavior of low carbon steel in 1M HCl solution at 25 °C is presented in Figure 6. The curves show a similar type of Nyquist plots for low carbon steel in the presence of various concentrations of *allium sativum*. The existence of single semi-circle showed the single charge transfer process during dissolution which is unaffected by the presence of inhibitor molecules.

Deviations from perfect circular shape are often referred to the frequency dispersion of interfacial impedance, which arises due to surface roughness, impurities, dislocations, grain boundaries, adsorption of inhibitor, and formation of porous layers and in homogenates of the electrode surface [27, 28]. The electrical equivalent circuit model is shown in Figure 7. It used to analyze the

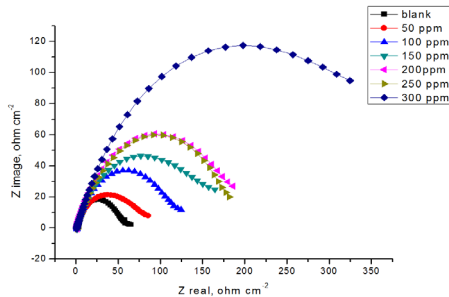


Fig. 6: The Nyquist plots for the corrosion of low carbon steel in 1M HCl in the absence and presence of different concentrations of *allium sativum* at 25 °C

obtained impedance data. The model consists of the solution resistance (R_s), the charge-transfer resistance of the interfacial corrosion reaction (R_{ct}) and the Constant phase element (CPE). Excellent fit with this model was obtained with our experimental data. The values of the interfacial capacitance C_{dl} can be calculated from CPE parameter values Y_0 and n using the expression [29]:

Equation 8:

$$C_{dl} = Y_0 (\omega_{max})^{n-1}$$

where Y_0 is the magnitude of the CPE, ω_{max} is the angular frequency at which the imaginary component of the impedance reaches its maximum values and n is the deviation parameter of the CPE: $-1 \leq n \leq 1$.

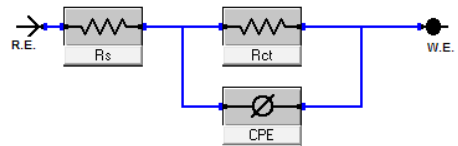


Fig. 7: Electrical equivalent circuit model used to fit the results of impedance

EIS data Table 7 show that the R_{ct} values increases and the C_{dl} values decreases with increasing the inhibitor concentrations. This is due to the gradual replacement of water molecules by the adsorption of the inhibitor molecules on the metal surface, decreasing the extent of dissolution reaction. The higher (R_{ct}) values, are generally associated with slower corroding system [30, 31].

3.7. Electrochemical frequency modulation (EFM) measurements

The EFM is a nondestructive corrosion measurement technique that can directly give values of the corrosion current without prior knowledge of Tafel constants. Like EIS; it is a small ac signal.

Tab.7: EIS data of low carbon steel in 1 M HCl in the absence and presence of different concentrations of *allium sativum* at 25 °C

%IE	θ	C_{dl} $\mu\text{F cm}^{-2}$	R_{s} $\Omega \text{ cm}^2$	R_{ct} $\Omega \text{ cm}^2$	[inh] ppm
-----	-----	389	1.3	54.3	Blank
27.5	0.275	330	1.2	74.9	50
53.4	0.534	323	1.2	116.6	100
64.9	0.648	320	1.2	154.7	150
70.3	0.703	312	1.3	183.1	200
70.5	0.705	275	1.2	184.2	250
85.5	0.854	270	1.1	374.4	300

It is generally accepted that in most cases, the corrosion rates determined with the EFM technique, are much higher than the values determined with other techniques exhibiting low corrosion rates [32]. The modulation frequencies that are used in the EFM technique are in the capacitive region of the impedance spectra.

The calculated corrosion kinetic parameters at different concentrations of *allium sativum* in 1 M HCl

at 25 °C (i_{corr} , β_a , β_c , CF-2, CF-3 and % IE) are given in Table 8. From Table 8, the corrosion current densities decrease by increasing the concentration of investigated compound and the efficiency of inhibition increases by increasing investigated compound concentrations. The causality factors in Table 8 are very close to theoretical values which according to EFM theory [33] should guarantee the validity of Tafel slopes and corrosion current densities. Values of causality factors in Table 8 indicate that the measured data are of good quality. The standard values for CF-2 and CF-3 are 2.0 and 3.0, respectively. The deviation of causality factors from their ideal values might be due to the perturbation amplitude was too small or that the resolution of the frequency spectrum is not high enough. Another possible explanation is that the inhibitor is not performing very well. The obtained results showed good agreement of corrosion kinetic parameters obtained with the EFM, Tafel extrapolation and EIS methods.

3.8. Surface morphology

In order to verify if the investigated extract molecules are in fact adsorbed on low carbon steel surface, both scanning electron microscopy (SEM) and

Tab.8: Electrochemical kinetic parameters obtained by EFM technique for low carbon steel in the absence and presence of different concentrations of *allium sativum* in 1 M HCl at 25 °C.

% IE	θ	C.R mpy	CF-3	CF-2	β_c mV dec^{-1}	β_a mV dec^{-1}	i_{corr} $\mu\text{A cm}^{-2}$	[inh] ppm
-----	----	143.9	2.4	1.7	109	94	315.0	Blank
32.2	0.322	97.6	1.0	1.9	89	83	213.5	50
49.4	0.493	72.9	1.6	1.2	96	90	159.5	100
62.1	0.620	54.6	2.6	1.5	96	89	119.4	150
62.3	0.622	54.3	2.9	2.1	107	97	118.8	200
63.1	0.630	53.1	2.8	1.8	104	90	116.3	250
73.0	0.730	38.8	2.9	1.9	143	113	84.9	300

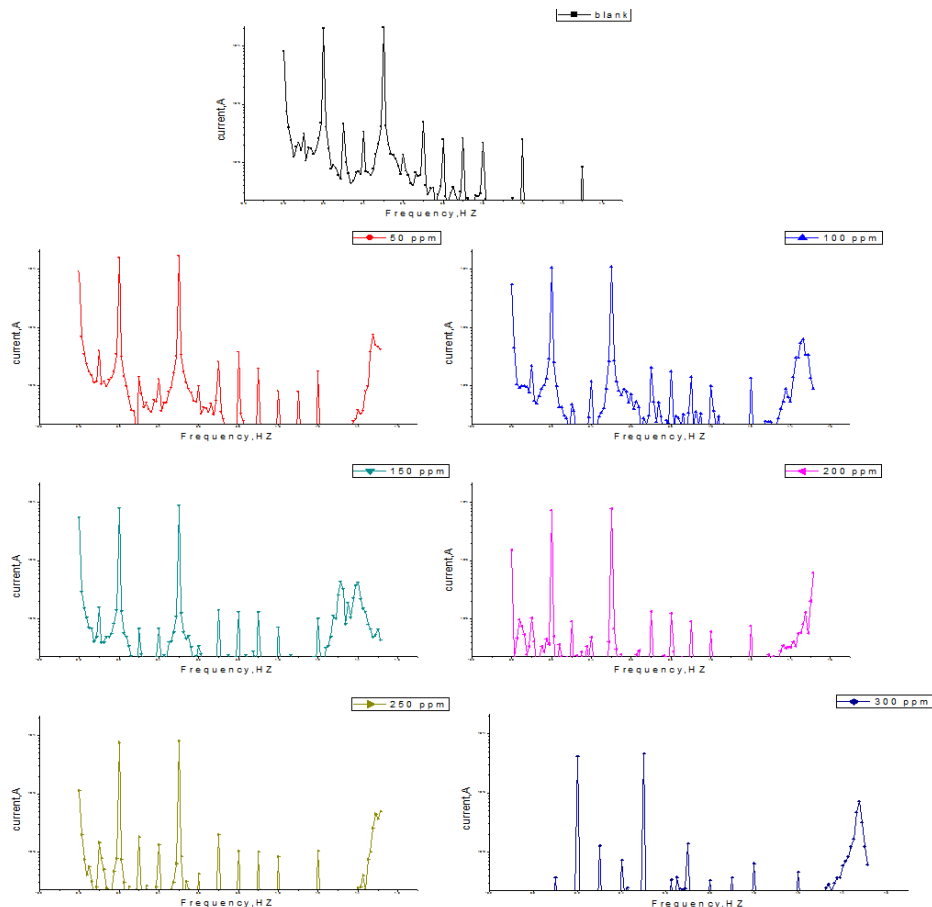


Fig.8: Intermodulation spectrum for low carbon steel in 1 M HCl solutions without and with various concentrations of *allium sativum* at 25°C

energy dispersive X-ray (EDX) experiments were carried out. The SEM micrographs for low carbon steel surface alone and after 24 h immersion in 1M HCl without and with the addition of 300 ppm of *allium sativum* are shown in Figures (9a-c). The corresponding EDX profile analyses are presented in Figures (10a-c). As expected, Figure 9a shows metallic surface is clear, while in the absence of the investigated compound, the low carbon steel surface is damaged by HCl corrosion Figure 9b. In contrast, in presence

of the investigated compound Figure 9c, the metallic surface seems to be almost no affected by corrosion. The corresponding EDX data are presented in Figures (10a-c) and Table 9. Figure 10c shows the EDX spectra of low carbon steel in the presence of investigated compound which suggest the adsorption of investigated compound on the low carbon steel surface and confirm the formation of a thin film of investigated compound observed in SEM micrograph, thus protecting the surface against corrosion.

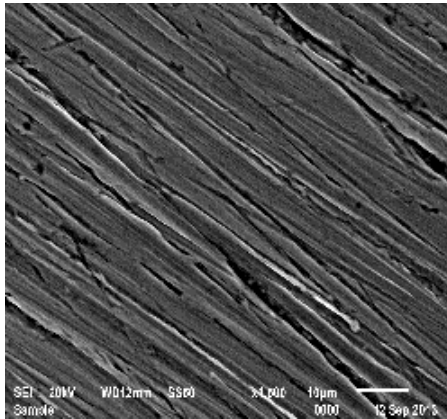


Fig.9a: SEM micrograph of low carbon steel surface before of immersion in 1 M HCl

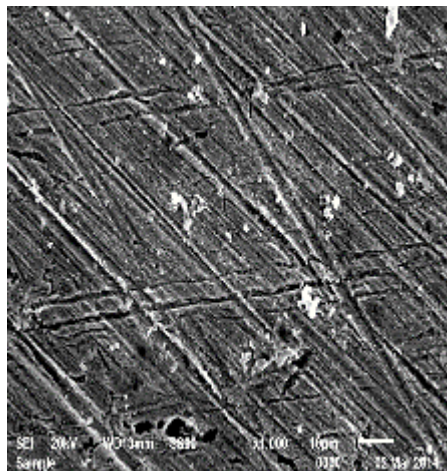


Fig.9b: SEM micrograph of low carbon steel surface after 24 h of immersion in 1 M HCl

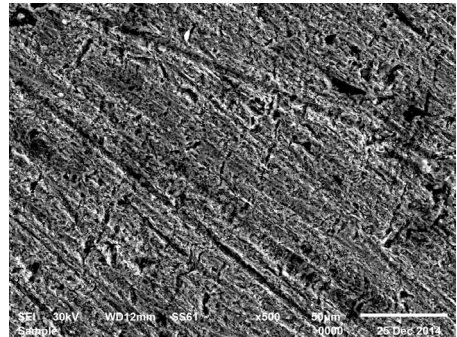


Fig.9c: SEM micrograph of low carbon steel surface after 24 h of immersion in 1 M HCl + 300 ppm of *allium sativum* at 25°C

4. Mechanism of Corrosion Inhibition

Results of the present study have shown that this extract inhibits the acid induced corrosion of low carbon steel by virtue of adsorption of its components such as organo-sulphur compounds (S-alkyl-L-cysteine sulfoxides (ACSOs), such as allicin, and g-glutamyl cysteines) [34] onto the metal surface. The inhibition process is a function of the metal, extract concentration, and temperature as well as inhibitor adsorption abilities which is so much dependent on the number of adsorption sites. The results show that the inhibition efficiency of *allium sativum* increases with increase in extract concentration suggesting that some of the molecules of the extract are adsorbed on the metal surface thereby protecting the “covered” surface from further corrodes attack. Increasing the extract concentration increases the degree of surface coverage, θ , of the metal surface.

Table 9: Surface composition (weight %) of low carbon steel before and after immersion in 1M HCl without and with 300 ppm of *allium sativum* at 25°C

(Mass %)	C	Cr	Ni	Si	Mn	P	S	Fe	O
Free	0.14- 0.20	0.1	0.01	0.24	0.5	0.05	0.05	rest	----
Blank	21.26	---	---	---	0.54	---	---	58.54	----
<i>allium sativum</i>	69.93	----	----	----	----	----	----	11.43	18.64

5. Conclusion

The possibility of using *allium sativum* extract as corrosion inhibitor for low carbon steel in 1M HCl has been evaluated. *Allium sativum* was

proved to be a good inhibitor. The inhibition efficiency increased as the concentration of *allium sativum* increased and hence corrosion rate decreased. The decrease in the corrosion rate by *allium sativum* extract was due to the forma-

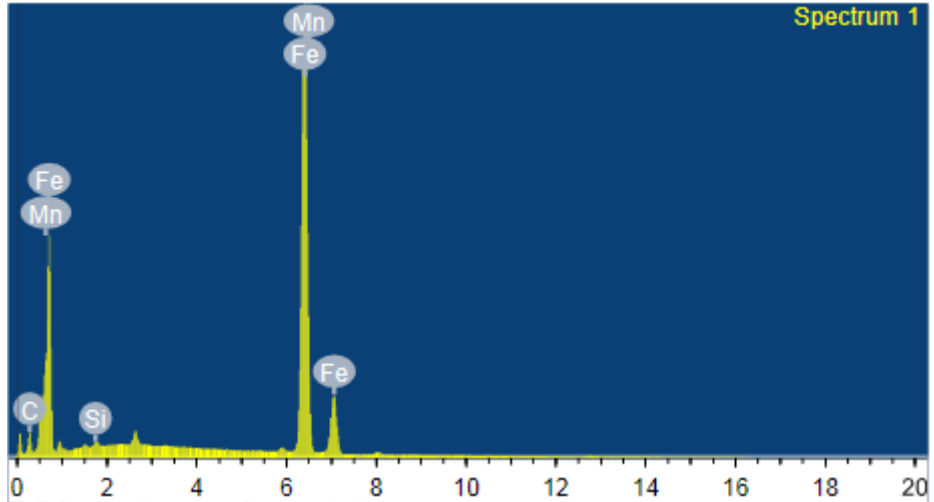


Fig.10a: EDX spectra of low carbon steel surface before of immersion in 1 M HCl

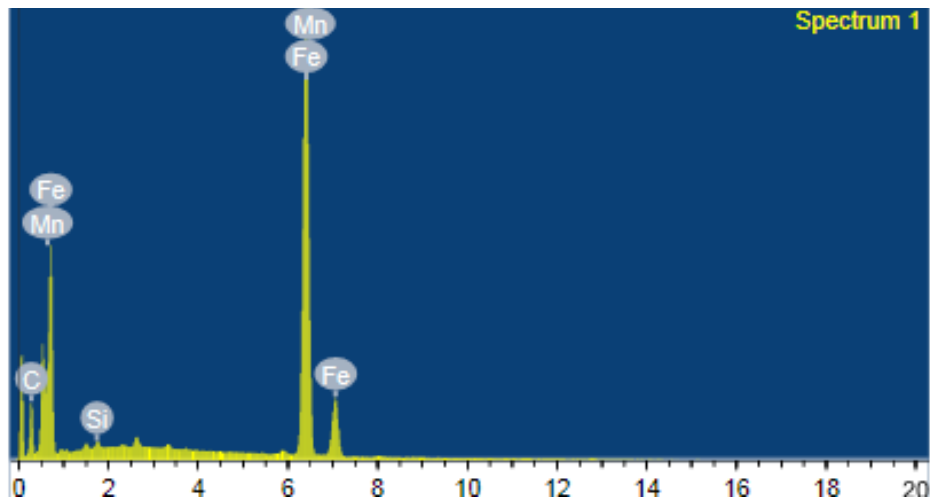


Fig.10b: EDX spectra of low carbon steel surface after 24 h of immersion in 1 M HCl

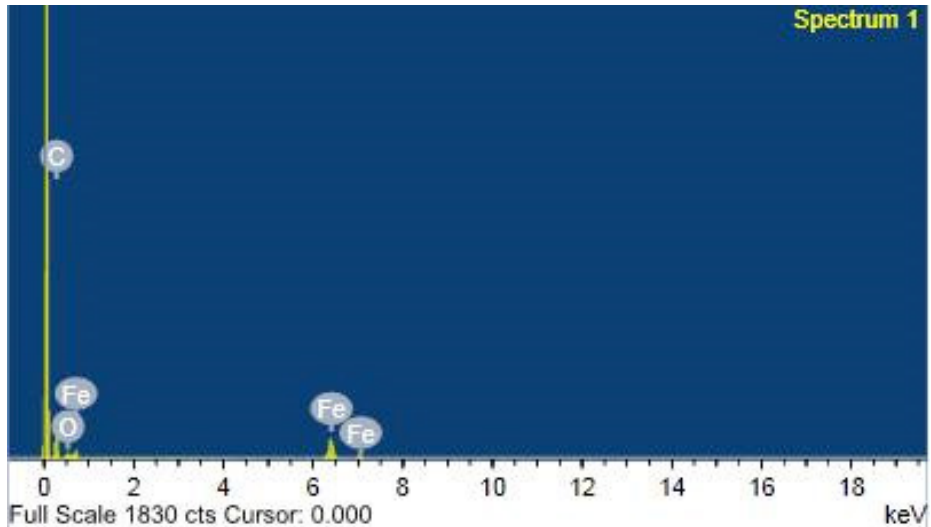


Fig.10c: EDX spectra of low carbon steel surface after 24 h of immersion in 1 M HCl + 300 ppm of *allium sativum* at 25°C

tion of a protective external film which contained compounds present in the garlic extract. *Allium sativum* acted mainly as a mixed type of inhibitor which was physically adsorbed on the low carbon steel surface.

References

- [1] E. A. Noor. Temperature effect on corrosion inhibition of mild steel in acidic solutions by aqueous extract of Fenugreek leaves, *Int J Electrochem Sci.* vol 2 p. 996-1017, 2007
- [2] R. Subha, R. Saratha. Naturally Occurring Substance (*Calendula Officinalis*-Flower) as a Corrosion Inhibitor of Mild Steel in 1M HCl Solution, *J. Corros. Sci. Eng.* vol. 10, p. 1-8. Preprint 9, 2006
- [3] A. Y. El-Etre. Inhibition of acid corrosion of carbon steel using aqueous extract of olive leaves, *J Colloid Interf Sci.* vol. 311, p. 578-583, 2007
- [4] E. E. Oguzie. Corrosion inhibition of aluminium in acidic and alkaline media by *Sansevieria trifasciata* extract, *Corros. Sci.*, vol. 49, p.1527-1539, 2007
- [5] A. A. Rahim, E. Rocca, J. Steinmetz, M.J. Kassim, R. Adnan, S.M. Ibrahim. Mangrove tannins and their flavanoid monomers as alternative steel corrosion inhibitors in acidic medium, *Corros. Sci.* vol. 49, p. 402-417, 2007
- [6] E. E. Oguzie, A.I. Onuchukwu, P.C. Okafor, E.E. Ebenso. Corrosion inhibition and adsorption behaviour of *Ocimum basilicum* extract on aluminium, *Article Options and Tools, Pigm Resin Technol.* vol. 35(2), p. 63-70, 2006
- [7] A. Y. El-Etre, Z. El-Tantary. Inhibition of Metallic Corrosion Using Ficus Extract, *Port Electrochim Acta.* vol. 24(3), p. 347-356, 2006
- [8] I. B., Obot N.O. Obi-Egbedi. Ginseng Root: A new Efficient and Effective Eco-Friendly Corrosion Inhibitor for Aluminium Alloy of type AA 1060 in Hydrochloric Acid Solution, *Int J Electrochem Sci.* vol. 4, p. 1277-1288, 2009
- [9] S. A. Umoren, I.B. Obot, N.O. Obi-Egbedi, *Raphia hookeri* gum as a potential eco-friendly inhibitor for mild steel in sulfuric acid, *J Mate. Sci.* vol. 44, p. 274-279, 2009
- [10] S. A. Umoren, I.B. Obot, L.E. Akpabio, S.E. Etuk. Adsorption and corrosive inhibitive properties of *Vigna unguiculata* in alkaline and acidic media, *Pigm. Resin Technol.* vol. 37(2), p. 98-105, 2008
- [11] S. A. Umoren, I.B. Obot, E.E. Ebenso, N.O. Obi-Egbedi. Studies on the Inhibitive Effect of Exudate Gum from *Dacryodes edulis* on the Acid Corrosion of Aluminium, *Port Electrochim. Acta.* vol. 26, p.199-209, 2008
- [12] N. O. Eddy, B.I. Ita, N.E. Ibisji, E.E. Ebenso Experimental and Quantum Chemical Studies on the Corrosion Inhibition Potentials of 2-(2-Oxoindolin-3-Ylideneamino) Acetic Acid and Indoline-2,3-Dione, *Int J Electrochem Sci.* vol. 6, p. 1027-1044, 2011
- [13] G. N. Mu, T. P. Zhao, M. Liu, T. Gu: Effect of metallic cations on corrosion inhibition of an anionic surfactant for mild steel, *Corrosion*, vol. 52, p. 853-856, 1996.

- [14] M. Stern and A. L. Geary: Electrochemical polarization: I. A Theoretical analysis of the shape of polarization curves, *J. Electrochem. Soc.*, vol. 104, p. 56-63, 1957.
- [15] S. S. Abdel-Rehim, K. F. Khaled, N. S. Abd-Elshafi: Electrochemical frequency modulation as a new technique for monitoring corrosion inhibition of iron in acid media by new thiourea derivative, *Electrochim. Acta*, vol. 51, p. 3269-3277, 2006.
- [16] R. W. Bosch, J. Hubrecht, W. F. Bogaerts, B. C. Syrett: Electrochemical frequency modulation: A new electrochemical technique for online corrosion monitoring, *Corrosion*, vol. 57, p. 60-70, 2001.
- [17] B. G. Ateya, B. E. El-Anadouli, F. M. El-Nizamy: The adsorption of thiourea on mild steel, *Corros. Sci.*, vol. 24, p. 509-515, 1984.
- [18] I. Langmuir: The constitution and fundamental properties of solids and liquids. II. Liquids, *J. Am. Chem. Soc.*, vol. 39(9), p. 1848-1906, 1917.
- [19] K. Aramaki and M. Hackerman: Inhibition mechanism of medium-sized polymethyleneimine, *J. Electrochem. Soc.*, vol. 116, p. 568-574, 1969.
- [20] Libin Tang, Xueming Li, Lin Li, Guannan Mu, Guangheng Liu: The effect of 1-(2-pyridylazo)-2-naphthol on the corrosion of cold rolled steel in acid media: Part 2: Inhibitive action in 0.5 M sulfuric acid, *Chem. Phys.*, vol. 97, p. 301-307, 2006.
- [21] M. Ajmal, A. S. Mideen, M. A. Quraishi: 2-hydrazino-6-methyl-benzothiazole as an effective inhibitor for the corrosion of mild steel in acidic solutions, *Corros. Sci.*, vol. 36, p. 79-84, 1994.
- [22] F. Bentiss, M. Lebrini, M. Lagrenee: Thermodynamic characterization of metal dissolution and inhibitor adsorption processes in mild steel/2,5-bis(*n*-thienyl)-1,3,4-thiadiazoles/hydrochloric acid system, *Corros. Sci.*, vol. 47, p. 2915-2931, 2005.
- [23] D. C. Silverman and J. E. Carrico: Electrochemical Impedance Technique — A Practical Tool for Corrosion Prediction, *Corrosion*, vol. 44, p. 280-287, 1988.
- [24] W. J. Lorenz and F. Mansfeld: Determination of corrosion rates by electrochemical DC and AC methods, *Corros. Sci.*, vol. 21, p. 647-672, 1981.
- [25] D. D. Macdonald and M. C. Mckubre: Impedance measurements in Electrochemical systems, *Modern Aspects of Electrochemistry*, J.O'M. Bockris, B.E. Conway, R.E. White, Eds., vol. 14, Plenum Press, New York, New York, p. 61, 1982.
- [26] C. Gabrielli: Identification of Electrochemical processes by Frequency Response Analysis, *Solartron Instrumentation Group*, 1980.
- [27] E. Bayol, K. Kayakirilmaz, M. Erbil: The inhibitive effect of hexamethylenetetramine on the acid corrosion of steel, *Mater. Chem. Phys.*, vol. 104, p. 74-82, 2007.
- [28] O. Benalli, L. Larabi, M. Traisnel, L. Gengembra, Y. Harek: Electrochemical, theoretical and XPS studies of 2-mercapto-1-methylimidazole adsorption on mild steel in 1 M HClO₄, *Appl. Surf. Sci.*, vol. 253, p. 6130-6139, 2007.
- [29] C. H. Hsu, F. Mansfeld: Concerning the Conversion of the Constant Phase Element Parameter Y₀ into a Capacitance, *Corrosion*, vol. 57, p. 747-749, 2001.
- [30] I. Epelboin, M. Keddam, H. Takenouti: Use of impedance measurements for the determination of the instant rate of metal corrosion, *J. Appl. Electrochem*, vol. 2, p. 71-79, 1972.
- [31] J. Bessone, C. M. K. Jüttner, and W. J. Lorenz: AC-impedance measurements on aluminium barrier type oxide films, *Electrochimica Acta*, vol. 28(2), p. 171-175, 1983.
- [32] E. Kuş and F. Mansfeld: An Evaluation of the Electrochemical Frequency Modulation (EFM) Technique, *Corros. Sci.*, vol. 48, p. 965, (2006).
- [33] GamryEchem Analyst Manual, 2003.
- [34] Laurian Vlase, Marcel Parvu, Elena Alina Parvu and Anca Toiu, Chemical Constituents of Three *Allium* Species from Romania, *Molecules*, vol. 18, p. 114-117, 2013

Authors

Prof. Dr. A. S. Fouda
Department of Chemistry, Faculty of Science,
El-Mansoura University
El-Mansoura-35516, Egypt
Email: asfouda@hotmail.com; asfouda@mans.edu.eg
Tel: +2 050 2365730
Fax: +2 050 2202281



S. M. Ghoneim
Department of Chemistry, Faculty of Science,
El-Mansoura University
El-Mansoura-35516, Egypt



A.A. Attia
Department of Chemistry, Faculty of Science,
Zagazig University,
Zagazig, Egypt
Email: azaattia91@yahoo.com

CONTACT:

EUGEN G. LEUZE VERLAG KG
Ralf Schattmaier
Karlstraße 4
88348 Bad Saulgau
Germany

Email: ralf.schattmaier@leuze-verlag.de
Phone: +49 0 7581 4801-12
Fax: +49 0 7581 4801-10